Articles in PresS. Am J Physiol Gastrointest Liver Physiol (January 7, 2010). doi:10.1152/ajpgi.00414.2009

The impact of elevation of total bilirubin level and etiology of the liver disease on serum *N*-glycosylation patterns in mice and men

Bram Blomme[(1)], Christophe Van Steenkiste[(1)], Jacques Vanhuysse[(2)], Isabelle Colle[(1)], Nico Callewaert[(3,4)], Hans Van Vlierberghe[(1)]

[(1)] Department of Hepatology and Gastroenterology, Ghent University Hospital, Ghent, Belgium
[(2)] Department of Pathology, Ghent University Hospital, Ghent, Belgium
[(3)] Unit for Molecular Glycobiology, Department for Molecular Biomedical Research, VIB, Ghent University, Ghent, Belgium
[(4)] Department of Biochemistry, Physiology and Microbiology, Ghent University, Ghent, Belgium

Contact Information

Prof. Dr. Van Vlierberghe Hans

Department of Hepatology and Gastroenterology

Ghent University Hospital

B-9000 Ghent, Belgium

Tel: +32 9 332 2370

Mail: Hans.Vanvlierberghe@UGent.be

Key-words: biomarker, glycomics, *N*-glycosylation, etiology, total bilirubin, α1-6 fucose

Abstract

The GlycoFibroTest and GlycoCirrhoTest are non-invasive alternatives for liver biopsy that can be used as a follow-up tool for fibrosis patients and to diagnose cirrhotic patients, respectively. These tests are based on the altered *N*-glycosylation of total serum protein. Our aim was to investigate the impact of etiology on the alteration of *N*-glycosylation and if other characteristics of liver patients could have an influence on *N*-glycosylation.

In human liver patients, no specific alteration could be found to make a distinction according to etiological factor, although alcoholic patients had a significant higher mean value for the GlycoCirrhoTest. Undergalactosylation did not show a significantly different quantitative alteration in the cirrhotic and non-cirrhotic population of all etiologies. Importantly, patients with an elevation of total bilirubin level (>2 mg/dl) had a strong increase of glycans modified with α1-6 fucose. The fucosylation-index was therefore significantly higher in fibrosis/cirrhosis and hepatocellular carcinoma patients with elevated total bilirubin levels irrespective from etiology. Furthermore, in a multiple linear regression analysis, only markers for cholestasis significantly correlated with the fucosylation-index.

In mouse models of chronic liver disease, the fucosylation-index was uniquely significantly increased in mice that were induced with a common bile duct ligation. Mice that were chronically injected with CCl_4 did not show this increase. Apart from this difference, common changes characteristic to fibrosis development in mice were observed. Finally, mice induced with a partial portal vein ligation did not show biological relevant changes indicating that portal hypertension does not contribute to the alteration of *N*-glycosylation.

1.Introduction

Liver fibrosis is characterized by the replacement of liver tissue by fibrous scar tissue and the development of regenerative nodules, leading to progressive loss of liver function (22). The 'golden' standard to asses progression of liver fibrosis is a liver biopsy (1,10), but is associated with several complications such as intraperitoneal haemorrhage (~1%), puncture of the gallbladder, pneumothorax (both <0.5%) and in very rare cases even death (0.01-0.001%) (18,20). Due to these limitations, there is an increasing demand for non-invasive serum tests and imaging techniques to assess the stage of liver fibrosis. In this regard, interest is raised in serum *N*-glycans profiles as potential indicator of liver disease.

The majority of serum proteins are produced by the liver and nearly all of these proteins are *N*-glycosylated, a noticeable exception being albumin. Recently, a new technological platform, DNA sequencer-assisted-fluorophore-assisted capillary electrophoresis (DSA-FACE) (14), has been developed to assess glycan structures. This has led to the discovery of a non-invasive test characteristic for end-stage cirrhosis, the GlycoCirrhoTest. This test is defined by the logarithmic proportion of the peak heights of a biantennary, α1-6 fucosylated and bisecting *N*-acetylglucosamine (GlcNAc) modified sugar (NA2FB - increased in cirrhosis) and a tri-antennary sugar (NA3 - decreased in cirrhosis) in the electropherogram (3).

NA2FB represents the increase of bisecting GlcNAc modified glycans in cirrhotic patients and NA3 represents the decrease of multi-antennary glycans in the serum of cirrhotic patients. This is associated with the up-regulation of *N*-acetylglucosaminyltransferase III (GnT-III - responsible for bisecting GlcNAc modified glycans) and the competitive decrease of *N*-acetylglucosaminyltransferase V (GnT-V - responsible for multi-antennary glycans) in regenerative nodules and these occur per definition only in the cirrhotic stage.

Undergalactosylation (UGS), the increase of agalacto glycans in serum, is also an important feature in the glycosylation patterns of liver patients. These glycans, that lack one or both galactoses, progressively increase with Metavir-stage (2) and they can be predominantly found on immunoglobulin G (IgG) (21).UGS of IgG forms the basis of the GlycoFibroTest . Finally, it was shown that the increased abundance of an α1-3 fucosylated glycan (NA3Fb) is associated with the development of HCC in HBV-patients (15).

Callewaert *et al* showed the potential of glycome research in biomarker discovery (3). Complementary to this study, we would like to investigate the impact of etiology on *N*-glycosylation patterns. Therefore, we examined five patient populations of different etiology: cholestatic, hepatitis B (HBV), hepatitis C (HCV), alcoholic and non-alcoholic steatohepatitis (NASH) patients and one control population of healthy volunteers. Importantly, it was observed that patients with an elevation in serum total bilirubin level (>2 mg/dl) had a significant increase of peak height of glycans modified with α1-6 fucose. Therefore, the fucosylation-index (FI), defined as the percentage of α1-6 fucosylated glycans in the glycome of serum proteins, was significantly elevated in fibrosis/cirrhosis patients with increased levels of total bilirubin. An increase of the FI has especially been linked with hepatocellular carcinoma (HCC)-patients (6,17), and therefore, we also tested some HCC-serum samples with normal (0-1 mg/dl) and elevated (>2 mg/dl) total bilirubin serum level. Moreover, patients with a strong elevation of total bilirubin level were excluded in the original studies [3,21,15].

To confirm the results of the human data, we investigated the *N*-glycosylation patterns of two mouse models of chronic liver disease, common bile duct ligation (CBDL) and subcutaneous injections with CCl_4. In addition, a mouse model for a pure portal hypertension (PHT) without liver damage, partial portal vein ligation (PPVL), was also evaluated.

2. Materials and methods

Human liver patients

Five patient populations of at least 15 patients were assembled (Table 1). Each group had a specific etiology: cholestasis (n=15), HBV (n=20), HCV (n=32), alcoholic (n=31) and NASH (n=17). The cholestatic group consisted out of 1 patient with progressive familial intrahepatic cholestasis, 9 patients with primary sclerosing cholangitis and 5 patients with primary biliary cirrhosis. Most of the alcoholic patients kept to a regime of alcohol abstinence at he time of analysis, there was only one active drinker (>21 alcoholic consumptions/week). The majority of HBV-patients (70%) were on treatment. We also included a control group of 16 healthy volunteers and a HCC-group of 16 patients (Table 2). The volume of the tumor in a HCC-patient was calculated based on the diameter (>1 cm) of the nodule(s) reported by the radiologist on CT-scan. In the case of multiple nodules, the different diameters were counted up. Subsequently, the formula to calculate the volume of a sphere ($4/3\pi r^3$) was used to assess tumor volume. Medical records of these patients were reviewed. Liver tests, Metavir-stage if determined by biopsy, other underlying diseases or conditions and clinical manifestations were assessed. All patients and volunteers signed an informed consent and the protocol was approved by the ethical committee of the Ghent University Hospital. Serum samples of patients and controls were taken fasted.

The concentration of bile acids in serum was spectrophotometrically determined on a Hitachi 912 analyser (Diagnostica; Boehringer Mannheim, Ingelheim, Germany) using a commercial kit (Trinity Biotech, Co Wicklow, Ireland). The alanine aminotransferase activity (ALT), aspartate aminotransferase activity (AST), gamma glutamyl transferase (GGT), alkaline phosphatase (AP), C-reactive protein (CRP), total bilirubin and total protein were analyzed using routine photometric test on a Hitachi 747 analyser (Diagnostica, Boehringer Mannheim, Ingelheim, Germany).

Animal models

Male C57Bl/6 mice (25-30 g) were purchased from Harlan Laboratories (Horst, The Netherlands). The mice were kept under constant temperature and humidity in a 12 hours controlled light/dark cycle. The Ethical Committee of experimental animals at the faculty of Medicine and Health Sciences, Ghent University, Belgium, approved the protocols.

The mouse model for a pure PHT without liver damage was induced by PPVL (7). The surgical procedure was performed under sterile conditions. Mice were anaesthetized under isoflurane inhalation (Forene®; Abbott NV, Brussels, Belgium). A midline abdominal incision was performed and the portal vein was separated from the surrounding tissue. A ligature (silk cut 5-0) was tied around both portal vein and adjacent 27-gauge blunt-tipped needle. Subsequent removal of the needle yielded a calibrated stenosis of the portal vein. Mice were sacrificed 7 and 14 days after PPVL (n=8 in each group).

The portal venous pressure was measured in PPVL and Sham mice. The portal vein was cannulated through an ileocolic vein with a 24-gauge catheter (Becton Dickinson, Erebodegem-Aalst, Belgium), which was advanced into the portal vein and connected to a highly sensitive pressure transducer (Powerlab, ADInstruments, Spechbach, Germany). The external zero reference point was placed at the midportion of the animal.

The mouse model for a secondary biliary cirrhosis is CBDL (13). The surgical procedure was performed under sterile conditions. Under isoflurane inhalation anaesthesia, a midline abdominal incision was made and the common bile duct was isolated. The common bile duct was occluded with a double ligature of a non-resorbable suture (silk cut 5-0). The first ligature was made below the junction of the hepatic ducts and the second was made above the entrance of the pancreatic duct. The common bile duct was sectioned between the two ligatures. Mice were sacrificed 1, 3, 4, 5 and 6

weeks after CBDL (n=8 in each group). Sham-operated mice were used as control group for the CBDL and PPVL model (n=8 in each group).

Finally, the third mouse model was induced by chronic subcutaneous (SC) administration of carbon tetrachloride (CCl_4) (Merck, Darmstadt, Germany) twice weekly (1:1 dissolved in olive oil; 1 ml/kg) (11). 5% alcohol was added to drinking water. Mice were sacrificed after 1, 3, 6, 10 and 16 weeks (n=8 per group). Control mice for CCl_4 received a saline solution (1ml/kg) subcutaneously (n=8 in each group). No alcohol was added to the drinking water. The time points at which the mice in the different mouse models were sacrificed roughly correspond with the semi-quantitative Metavir-stage (2) as validated in a previous study (8).

Blood samples were taken by puncture of the aorta abdominalis. These samples were centrifuged at 2000 rpm for 10 minutes. At least 200 µl serum was taken off the clot and the alanine aminotransferase activity (ALT), aspartate aminotransferase activity (AST) and total bilirubin were analyzed as described for the human samples. The remaining serum volume was used for the analysis of the *N*-glycan profiles and to perform two Enzyme-Linked Immuno Sorbant Assays (ELISA) for the determination of the serum IgG and Serum Amyloid A concentration (Immunology Consultants Laboratory, Inc – Newburg, OR, USA). The ELISAs were run according to manufacturer's instructions and all analyses were done in duplo.

Histopathology of the mouse liver was performed by staining with 0.1% picrosirius red. Microscopic evaluation was carried out blinded by two independent investigators (J.V. and B.B.). Scoring of the liver tissues was done to determine the stage of fibrosis and this was expressed according to the Metavir-score (2) with the emphasis on the fibrosis and not on activity.

Serum protein N-glycome sample processing

The 96-well on-membrane deglycosylation method (14) was used to prepare APTS-labeled *N*-glycans from 5 µl serum. Samples were finally reconstituted in 5 µl milliQ water and analyzed using DSA-FACE.

To get an idea about the structures of the glycans present in the mouse profiles, exoglycosidase array sequencing was applied. Batches (0.5 µl) of APTS-labeled *N*-glycans were subjected to digestion with different mixtures of exoglycosidases in 5 mM NH_4Ac (pH 5). The enzymes used were *Arthobacter ureafaciens* sialidase, *Streptococcus pneumoniae* β-1,4-galactosidase, jack bean β-*N*-acetylhexosaminidase and bovine kidney α-fucosidase. After complete digestion (overnight at 37°C), the samples were evaporated to dryness, reconstituted in 10 µl water and analyzed by DSA-FACE.

Data processing

We quantified the heights of 11 peaks that were detectable in all mouse and human samples (fig. 1) to obtain a numerical description of the profiles, and analyzed these data with SPSS 15.0 software (SPSS, Chicago, IL, USA). First, the sum of the peak heights of all the peaks were calculated (total intensity) and then the peak heights were normalized to the total intensity of the measured peaks (expressed as percentage of the total intensity).

All mouse data were analyzed with Mann-Whitney U-test (control vs. treated). The human data were statistically processed as appropriate for the study design (independent sample *t*-test, single-factor ANOVA, Kruskal-Wallis test and multiple linear regression). A *P*-value less than 0.05 was considered significant in all analyses.

3. Results

Alcoholic patients have a significant higher mean value for the GlycoCirrhoTest

The analysis was done on cirrhotic HCV (n=21) and cirrhotic alcoholic patients (n=23). The relative percentage of NA2FB was significantly higher in the alcoholic group compared to the HCV-group (8.9% ±2,8 vs. 6.4% ±2,4) (*P*=0.004, two-tailed *t*-test). The relative percentage of NA3 was not significantly different between the two groups (*P*=0,164, two-tailed *t*-test), although the mean value in the alcoholic group was lower than in the HCV-group (2,5% vs. 3,1%). As a consequence, the mean value of the GlycoCirrhoTest was almost double as high in the alcoholic group compared to the HCV-group (0.59 ±0,33 vs. 0,31 ±0,26) (*P*=0,005, two-tailed *t*-test). The cirrhotic patients in the other etiologies also had a mean value that was considerably lower than that of alcoholic patients: cholestatic (0.26 ±0.2 – n=4) and HBV (0.3 ±0.39 – n=9). These latter observations were still substantially higher in comparison with the control group (-0.03 ±0.15) (fig. 2). The value for NASH-patients (0.5 ±0.57 – n=4) was also quite high. Our data-set, in all etiologies together, had a AUROC of 0.81 for the discrimination between F0-F3 and F4 which was similar to the original study (3). More informative was the AUROC in the individual etiologies: cholestatic (0.77), HBV (0.72), HCV (0.68), alcoholic (0.96) and NASH (0.83). Finally, we found significant correlations between scores of the GlycoCirrhoTest and various markers of chronic liver disease: GGT, AST, total bilirubin, AP and bile acids (*P*<0,001; Spearman rank test) and ALT (*P*=0,018; Spearman rank test). This was expected because the GlycoCirrhoTest only displays an increase in score in the cirrhotic stage as these parameters were also seen to be elevated at this stage. In contrast, there was no correlation between scores of the GlycoCirrhoTest and viral load in HBV and HCV-patients (P=0,347; Spearman rank test).

No significantly different quantitative alteration in undergalactosylation score between all etiologies

Undergalactosylation (UGS) score was defined as [(2x(peak1+2)) + peak 3 + peak 4] / [2x(peak1 + peak2 + peak3 + peak4 + peak5 + peak6 + peak7)) + (3x(peak8 + peak9 + peak10)) + (4xpeak11)] (expressed in %) (20).

In the non-cirrhotic group (F1-F3), there was no significant difference in UGS score between the etiologies as determined by pairwise comparisons using Scheffé-tests (single-factor ANOVA). The HCV and alcoholic liver disease group showed the highest mean level of UGS score (0.24 and 0.23, respectively), followed by HBV (0.2), cholestatic liver disease (0.18) and NASH (0.16). (*P*=0,322)

The classification according to Metavir-stage was possible for the HCV-population (table 1). We were able to reproduce the linear increase of UGS score in increasing Metavir-stage: F1: 0.15, F2: 0.25, F3: 0.29 and F4: 0.32.

In cirrhotic patients, again no significant difference in UGS score between the etiologies was seen (*P*=0.054 – Kruskal-Wallis H test). Mean UGS score was highest in cirrhotic NASH patients (0.35), followed by alcoholic (0.34) and HCV (0.32) patients. Cholestatic (0.23) and HBV (0.17) patients had a clearly lower, although not significant, mean level of UGS score.

Fucosylation-index is significantly increased in fibrosis/cirrhosis and HCC-patients with an elevation of total bilirubin level

It was observed that the FI of liver patients with an elevation in total bilirubin level (70%) was significantly higher than the FI of liver patients with normal total bilirubin levels (52.9%) (*P*<0.001, two-tailed *t*-test). The increase in α1-6 fucosylation was clearly not linked to etiology (single-factor ANOVA, *P*=0,254), only to an elevation in total bilirubin level. The FI was comparable in the progression of F1 to F3 in HCV-patients (0.5, 0.58 and 0.52, respectively), but it was clearly elevated

242 in the cirrhotic stage (0.7). Patients with the syndrome of Gilbert had a normal FI. The degree of α1-3
243 fucose did not differ significantly between patients with normal and elevated bilirubin levels
244 (*P*=0.687, two-tailed *t*-test).

245 We also tested other markers of liver damage (AST, ALT, GGT, AP, CRP and total protein) to
246 investigate if these did not confound our results. Only AST and AP were also significantly elevated in
247 the group with increased FI (*P*=0.001 and *P*=0.034, respectively, two-tailed *t*-test).

248 Subsequently, we tested eight HCC-patients with an elevation in total bilirubin level and eight HCC-
249 patients with normal total bilirubin level. Again, the FI in the HCC-group with elevated total bilirubin
250 concentrations was significantly higher (70.8% vs. 48.7% - *P*<0.001, two-tailed *t*-test). Both
251 populations did not differ in AFP-level (*P*=0.35, two-tailed *t*-test) but AST was significantly increased
252 in the HCC-group with increased FI (*P*<0.001, two-tailed *t*-test) in agreement with the results in the
253 fibrosis/cirrhosis group. There was no significant difference in the other markers (ALT,GGT, AP, CRP
254 and total protein). Again, the level of α1,3-fucose did not differ significantly between HCC-patients
255 with normal and elevated bilirubin levels (*P*=0.585, two-tailed *t*-test).

256 We also analyzed the correlation between the scores of the GlycoHCCTest and tumor volume in
257 HCC-patients. There was a clear trend observed between the two variables, but significance was not
258 reached (*P*=0,054; Spearman rank test). Only 1 HCC-patient showed metastasis and this did not
259 influence the score.

260 *Serum bile acid concentration*

261 Serum bile acid concentration was determined in every fibrosis/cirrhosis and HCC-patient.
262 Inconsistent data (low total bilirubin, high FI and vice versa) showed consistency in the bile acid data.
263 Cholestatic patients had a mean serum bile acid concentration of 49.5 µmol/L (±83.4), HBV-patients
264 had a mean value of 16.2 µmol/L (±26.1), HCV-patients had a mean value of 38.6 µmol/L (±53.2),

alcoholic patients had a mean value of 50.2 µmol/L (±56), NASH-patients had a mean value of 67.2 µmol/L (±85.4) and HCC-patients had a mean value of 51.5 µmol/L (±73).

Only markers for cholestasis correlated significantly with the FI in a multivariate analysis

The total bilirubin and bile acid data were first logarithmically transformed. The correlation between the FI and the discontinuous variables HCC, cirrhosis (cirrhotic and non-cirrhotic) and etiology was determined with a two-tailed Spearman test and a single-factor ANOVA. The correlation with the continuous variables total bilirubin, serum bile acid concentration, AST and AP was determined with a simple linear regression analysis. The variables AST, total bilirubin, serum bile acid concentration and cirrhosis correlated significantly with the FI (P<0.001). Scatter dots of the correlation between the (logarithmically transformed) total bilirubin and serum bile acid concentration are seen in figure 3.

Subsequently, a multiple linear regression analysis was performed with FI as dependent factor and bilirubin level, serum bile acid concentration, AST, AP, HCC, etiology and cirrhosis as co-variants in the linear model. The (logarithmically transformed) total bilirubin level, (logarithmically transformed) bile acid concentration and AP correlated significantly with the FI (P<0.001, P=0.001 and P=0.029, respectively) in the linear model.

Laboratory tests and histological analysis of mouse models of chronic liver disease

Test samples (4 in the PPVL and Sham group) confirmed earlier reports that there were no changes in AST, ALT and bilirubin after PPVL induction (6). One week after PPVL induction, the portal venous pressure (PVP) was at a mean of 8.3 mmHg (±1.9) and two weeks after PPVL induction, mean PVP rose further to 10.7 mmHg (±4). This was significantly higher than sham-operated mice that had a mean PVP of 4.3 mmHg (±0.8) (P<0.001) one week after induction and at 2 weeks a PVP of 5 mmHg (±1.7) (P=0.004). Histological examination revealed no significant fibrosis development in PPVL mice at 1 and 2 weeks after induction. They were predominantly scored F0.

After 3 weeks of CCl_4 administration, the Sirius Red stain demonstrated fibrotic changes in the centrolobular area. After 6 weeks, the liver architecture demonstrated a reversed lobulation due to development of centro-central fibrotic linkages and after 10 weeks, the reversed lobulation was accentuated with the development of centro-portal thin fibrotic septa apart from the centro-central fibrotic linkages. Finally, after 16 weeks, all mice had homogeneous characteristics of cirrhosis. For laboratory tests see table 3.

Enlargement of the portal tracts accompanied by dilatation of bile canaliculi and proliferation of the smaller bile ducts appeared as soon as 1 week after CBDL. After 3 weeks, the periportal alterations were accompanied by fibrotic changes to be described as F2 and evolving into F3 after 5 weeks of CBDL. After 6 weeks, the majority of mice (62,5%) developed cirrhosis with nodular changes in the liver parenchyma. For laboratory tests see table 3. Typical cirrhotic images of CBDL and CCl_4 mice are seen in figure 4.

N-glycosylation patterns in mouse models of chronic liver disease

The overall picture of the glycosylation pattern of a PPVL mouse was that of a control sample. One week after PPVL induction, peak 5/NA2 was significantly decreased (*P*=0.003) and peak 6 was significantly increased (*P*=0.006) compared to sham mice. Two weeks after induction, when PVP is at its maximum (7), only one peak was significantly altered: peak 9 was significantly increased (*P*=0.004) compared to Sham mice (Table 4). However no systematic changes were observed.

In CCl_4 mice, a significant increase in peaks 9 and 11 in the glycosylation pattern was observed starting from the first week of CCl_4 treatment. Peak 10 also started to increase significantly in abundance from 6w on. After three weeks CCl_4, peak 5/NA2 decreased significantly in abundance and at later time points, its two adjacent peaks (peak 3 and 4) also decreased significantly in abundance (fig. 5) (*P*-values see Table 4).

CBDL mice were characterized by the significantly increased abundance of peaks 1, 6 and 7 (table 4, fig. 5) in the glycosylation pattern. Peak 1/NGA2F increased significantly already in the first week after CBDL, peaks 6 and 7/NA2F after 3 weeks CBDL. Fucosidase digest revealed that these are all fucosylated glycans. CBDL mice also exclusively had a significant lowered abundance of peak 8 and, common with CCl_4, a decrease in abundance of peaks 4 and 5/NA2. CBDL mice also showed a significantly elevated peak height of peaks 9, 10 and 11 in agreement with CCl_4 mice. Peak 11 was significantly increased in abundance from an early stage on, but peaks 9 and 10 only in the cirrhotic stage (*P*-values see Table 4).

As a consequence of the increase of fucosylated glycans in CBDL mice, the FI was an excellent marker to distinguish CCl_4 and CBDL mice. This index barely rose above 20% in CCl_4 and control mice, while it reaches 30 to 40% in CBDL mice ($P<0.001$ in F2, F3 and F4-stage) (fig. 6). We also analyzed one pure bile mouse sample and the FI was comparable to a serum sample of a CBDL mouse (42%).

IgG and SAA concentration in mouse models of chronic liver disease

Six mice were evaluated at every time point in the CCl_4 and CBDL group and two mice at every time point in the control mice. Both fibrotic mouse models showed a doubling of the IgG concentration in the progression of fibrosis to cirrhosis (from approx. 0.5 mg/ml to approx. 1.3 mg/ml). Apart from an early strong increase in SAA-concentration (a mean of 700 µg/ml after 3w in the CCl_4 model and a mean of 320 µg/ml after 1w in the CBDL model) no significant difference in SAA-concentration between the CCl_4, CBDL and control mice could be observed (baseline value was approximately 50 µg/ml).

4. Discussion

Alteration of total serum *N*-glycans is indicative for chronic necro-inflammatory diseases and especially in liver diseases, it shows great potential as biomarker (3,21,15). Our group has made

335 important contributions to this research with a follow-up tool for fibrosis (21) and non-invasive tests
336 for cirrhosis and HCC (3,15).

337 Alcoholic patients were shown to have a mean value for the GlycoCirrhoTest that was considerably
338 higher than in other liver patients. This could be due to the micronodular fibrotic nature of the liver
339 of alcoholic patients. More nodules correspond to more elevated GnT-III induction in the cirrhotic
340 liver (3). The mean value of NASH-patients was also quite high, but this was due to one outliner in a
341 limited number of samples. Nevertheless, the mean value of the cirrhotic patients in all etiologies
342 was significantly and considerably higher than the mean value of the control group. (4) stated that
343 NASH-patients had no change in expression of GnT-III and GnT-V and these patients could therefore
344 not be diagnosed with the GlycoCirrhoTest. However, we found that three out of our four cirrhotic
345 NASH patients had a high value for the GlycoCirrhoTest, well over the cut-off value for cirrhosis,
346 which implies strong up-regulation of GnT-III and concomitant down-regulation of GnT-V. (fig. 2).

347 UGS of IgG in the progression of fibrosis is the feature on which the GlycoFibrotest is mainly based.
348 This paper shows that there was no significantly different quantitative alteration in
349 undergalactosylation in the cirrhotic as well as in the non-cirrhotic population across all etiologies
350 (fig. 2). Remarkable was the strong increase of UGS score in cirrhotic NASH-patients compared to the
351 non-cirrhotic group. The overall higher mean value of UGS in the cirrhotic stage (with the exception
352 of HBV) can be attributed to the linear increase of the mean UGS state of IgG that reaches a
353 maximum in end-stage liver disease (21) as exampled in HCV-patients.

354 An important finding was that an elevation of total bilirubin is strongly associated with a consequent
355 increase of the FI. In a multiple regression model, a significant correlation was found with the
356 (logarithmically transformed) bile acid concentration and AP. These biochemical variables are
357 markers for liver damage, but specifically for cholestasis.

Increase in fucosylation has especially been linked with HCC and an up-regulation of fucosyltransferases in hepatoma tissue was suggested to be the driving force after this increased fucosylation of serum proteins (18,5). An alternative hypothesis in non-HCC cholestatic patients reasons that α1-6 fucosylation of *N*-linked glycans within polarized hepatocytes directs glycoproteins to the basolateral surface and into bile. As a consequence, α1-6 fucosylated glycoforms are normally rare in the blood, and are enriched in the bile. Thus, if liver cells become depolarized, the α1-6 fucosylated glycoforms rise in abundance in the blood (16). The data collected in this study strongly favors the latter hypothesis. Moreover, the presence of high concentrations of bile acids in the serum samples with high FI is a strong confirmation of our data.

In the setting of cholestasis, the basolateral path to the bile ducts is blocked. Therefore, we hypothesize that there is an accumulation of α1-6 fucosylated glycoproteins in the hepatocyte. The only exit for these glycoproteins is apically to the Space of Disse and eventually to the systemic circulation. In conclusion, α1-6 fucosylation does not seem to be a HCC marker, but a marker for cholestasis.

Our group has previously shown that α1-3 fucose significantly increases in HCC-patients (15). However, we could not reproduce this up-regulation of α1-3 fucose. Possibly because we used a mixed HCC-population of different etiologies in contrast to the original study that was uniquely performed in HBV-patients (15). α1-3 fucose did not differ significantly between patients with normal and elevated bilirubin level, both in fibrosis/cirrhosis and HCC-patients.

The mouse models allowed us to investigate some variables independently from each other. The influence of PHT was investigated with PPVL mice. No biologically relevant changes in *N*-glycosylation were observed in the PPVL mice indicating that PHT does not contribute to the alteration of *N*-glycosylation in liver diseases.

The effect of elevated total bilirubin levels on *N*-glycosylation can be studied with CBDL mice. In analogy with liver patients that had a strong increase in total bilirubin, CBDL mice had a strong increased abundance of all α1-6 fucosylated glycans. An additional advantage of mouse models is the easy follow-up of histology and there is also less bias in the histological analysis of the mouse liver. In this respect, we were able to observe that the increase of α1-6 fucosylation is an early event in the cholestatic development (table 3).

CCl_4 mice did not show an increase in total bilirubin level and these mice therefore did not have an increased FI. These mice develop a micronodular fibrosis/cirrhosis with characteristics of an alcoholic cirrhosis and it is also considered as a model with an important amount of inflammation. However, inflammation did not have an influence on the *N*-glycosylation patterns in these mouse models. Apart from an early peak in SAA-concentration, no significant difference was observed and there was no such correlation with the *N*-glycosylation patterns of the mouse models. The hallmarks of CCl_4 mice are an increase of peaks 9, 10 and 11, probably all multi-antennary glycans. Again, this occurred very early in the fibrotic development and was not unique to CCl_4 mice because also CBDL mice had a significant increased abundance of these three glycans, albeit later in the fibrotic development. Other common changes with CBDL were a significant decrease in abundance of peak 5/NA2 and its adjacent peak 4.

Some *N*-glycosylation aspects of human liver patients are difficult to study in mouse models. Even if UGS would be present in mouse models, it would be much less pronounced than in humans because the IgG-concentration in serum is inherently low at 0,5 to 1,5 mg/dl. Additionally, in mice, glycan modifications that do not exist in humans, especially α-galactosylation, are present (12). Therefore, the baseline *N*-glycosylation pattern of a control C57Bl/6 mouse will be different than the baseline *N*-glycosylation pattern of a healthy human control (fig. 1). Moreover, our study strongly suggests that the spectrum of *N*-glycosylation alterations in liver disease is different between mouse and man. In summary, caution is offered when extrapolating mouse data.

In conclusion, we have shown that the GlycoFibroTest and GlycoCirrhoTest can be used in all etiologies as universal non-invasive tests. An important finding was that liver patients with elevated total bilirubin levels have a significant increase of glycans modified with α1-6 fucose. When studying fucosylation, a distinction has to be made between an increase of α1-6 fucose which is a marker for cholestasis and an increase of α1-3 fucose which is a marker for HCC, the latter most likely exclusively in HBV-patients. Future studies on biomarker discovery based on *N*-glycosylation will have to take into account that an increase of total bilirubin is attended with an increase of α1-6 fucosylation in serum.

Acknowlegdements

The authors wish to thanks Julien Dupont, Kim Olievier and Annelies Van Hecke for their expert technical assistance and Dieter Vanderschaeghe for editing the manuscript and for the helpful discussions.

REFERENCES

1. **Al Knawy B, Shiffman M.** Percutaneous liver biopsy in clinical practice. *Liver Int* 27:1166-1173, 2007.
2. **Bedossa P, Poynard T.** An algorithm for the grading of activity in chronic hepatitis C. The METAVIR Cooperative Study Group. *Hepatology* Aug;24(2):289-293, 1996.
3. **Callewaert N, Van Vlierberghe H, Van Hecke A, Laroy W, Delanghe J, Contreras R.** Noninvasive diagnosis of liver cirrhosis using DNA sequencer-based total serum protein glycomics. *Nature Medicine* 10:429-434, 2004.
4. **Chen, C., Schmilovitz-Weiss, H., et al.** Serum Protein N-Glycans Profiling for the Discovery of Potential Biomarkers for Nonalcoholic Steatohepatitis. *J Proteome Res* 8, 463-470, 2009.
5. **Chen G, Guan M, Su B, Lu Y.** mRNA expression of three glycosyltransferases in human hepatoma tissues. *Clin Chim Acta* 313(1-2):77-80, 2001.
6. **Comunale, M.A., Lowman, M., et al.** Proteomic analysis of serum associated fucosylated glycoproteins in the development of primary hepatocellular carcinoma. *J Proteome Res* 5, 308-315, 2006.
7. **Fernandez M, Vizzutti F, Garcia-Pagan J, Rodes J, Bosch J**. Anti-VEGF Receptor-2 monoclonal antibody prevents portal-systemic collateral vessel formation in portal hypertensive mice. *Gastroenterology* 126:886-894, 2004.
8. **Geerts AM, Vanheule E, Praet M, Van Vlierberghe H, De Vos M, Colle I.** Comparison of three research models of portal hypertension in mice: macroscopic, histological and portal pressure evaluation. *Int J Exp Path* 89:251-263, 2008.
9. **Gilmore IT, Burroughs A, Murraylyon IM, Williams R, Jenkins D, Hopkins A.** Indications, Methods, and Outcomes of Percutaneous Liver-Biopsy in England and Wales - an Audit by the British-Society-of-Gastroenterology and the Royal-College-of-Physicians-of-London. *Gut* 36:437-441, 1995.
10. **Grant A, Neuberger J.** Guidelines on the use of liver biopsy in clinical practice. *Gut* 45:S1-S11, 1999.
11. **Janakat S, Al-Merie H.** Optimization of the dose and route of injection, and characterization of the time course of carbo tetrachloride-induced hepatotoxicity in the rat. J Pharmacol *Toxicol Methods* 48, 41-44, 2002.
12. **Koike C, Uddin M, Wildman DE, Gray EA, Trucco M, Starzl TE, Goodman M.** Functionally important glycosyltransferase gain and loss during catarrhine primate emergence. *PNAS* 104:559-564, 2007.
13. **Kountouras J, Billing BH, Scheuer PJ**. Prolonged bile duct obstruction: a new experimental model for cirrhosis in rat. *Br J Exp Pathol* 65, 305-311, 1984.
14. **Laroy W, Contreras R, Callewaert N.** Glycome mapping on DNA sequencing equipment. *Nature Protocols* 1:397-405, 2006.
15. **Liu XE, Desmyter L, Gao CF, Laroy W, Dewaele S, Vanhooren V, Wang L, et al.** N-glycomic changes in hepatocellular carcinoma patients with liver cirrhosis induced by hepatitis B virus. *Hepatology* 46:1426-1435, 2007.
16. **Nakagawa T, Uozumi N, Nakano M, Mizuno-Horikawa Y, Okuyama N, Taguchi T, et al.** Fucosylation of N-glycans regulates the secretion of hepatic glycoproteins into bile ducts. *J Biol Chem* 281(40):29797-29806, 2006.
17. **Noda K, Miyoshi E, Uozumi N, Yanagidani S, Ikeda Y, Gao CX, et al.** Gene expression of alpha 1-6 fucosyltransferase in human hepatoma tissues: A possible implication for increased fucosylation of alpha-fetoprotein. *Hepatology* 28(4):944-952, 1998.
18. **Ohno M, Nishikawa A, Koketsu M, Taga H, Endo Y, Hada T, et al.** Enzymatic basis of sugar structures of alpha-fetoprotein in hepatoma and hepatoblastoma cell lines: correlation with activities of alpha 1-6 fucosyltransferase and N-acetylglucosaminyltransferases III and V. *Int J Cancer* 8;51(2):315-317, 1992.

19. **Piccinino F, Sagnelli E, Pasquale G, Giusti G.** Complications Following Percutaneous Liver-Biopsy - a Multicenter Retrospective Study on 68 276 Biopsies. *J Hepatol* 2:165-173, 1986.
20. **Van Beneden K, Coppieters K, Laroy W, De Keyser F, Hoffman IE, Van den Bosch F et al.** Reversible changes in serum immunoglobulin galactosylation during the immune response and treatment of inflammatory autoimmune arthritis. *Ann Rheum Dis* 68(8):1360-5, 2009.
21. **Vanderschaeghe, D., Laroy, W., et al.** GlycoFibroTest is a highly performant liver fibrosis biomarker derived from DNA sequencer-based serum protein glycomics. *Moll Cell Proteomics* 8(5), 986-94, 2009.
22. **Wallace K, Burt AD, Wright MC.** Liver fibrosis. *Biochemical Journal* 411:1-18, 2008.

Fig. 1. The upper panel shows a typical desialylated *N*-glycan profile from a control C57Bl/6 mouse total serum protein. The lower panel shows a typical desialylated *N*-glycan profile from a healthy human control total serum protein. The glycan structures of all the peaks in the human profile are known: Peak 1 indicates an agalacto α1-6 fucosylated biantennary glycan (NGA2F), peak 2 indicates an agalacto α1-6 fucosylated bisecting biantennary glycan (NGA2FB), peaks 3 and 4 indicate a single agalacto α1-6 fucosylated biantennary glycan (NG1A2F), peak 5 indicates a bigalacto biantennary glycan (NA2), peak 6 indicates a bigalacto α1-6 fucosylated biantennary glycan (NA2F), peak 7 indicates a bigalacto α1-6 fucosylated bisecting biantennary glycan (NA2FB), peak 8 indicates a tri-antennary glycan (NA3), peak 9 indicates a α1-3 fucosylated triantennary glycan (NA3Fb), peak 10 indicates a α1-6 fucosylated triantennary glycan (NA3Fc) and peak 11 indicates a tetra-antennary glycan (NA4). The symbols used in the structural formulas are as follows: (○) β-linked galactose, (□) β-linked N-acetylglucosamine, (●) α/β-linked mannose, (▶) α-1,3/6-linked fucose. The structures of the peaks in the mouse profile were obtained after exoglycosidase digests. The three glycans indicated in the murine profile were clearly deduced from the exoglycosidase digests (data not shown).

Fig. 2. Comparison of typical cirrhotic *N*-glycan profiles of different etiologies and a typical *N*-glycan profile of a healthy control. The peaks that represent undergalactosylated glycans are in red and the peaks that represent the GlycoCirrhoTest are in green.

Fig. 3. Scatter dots of the correlation between the logarithmically transformed bilirubin and serum bile acid concentration with the fucosylation-index.

Fig.4 Sirius Red staining (objective magnification 10x). A) control mice for CCl_4 and Sham-operated mice did not develop fibrosis at any time point (Stage 0 or F0). B) Typical cirrhotic image of the liver 6 weeks after common bile duct ligation (black arrow: fibrotic strands, white arrow: bile duct proliferation). C) Typical cirrhotic image of the liver chronically injected with CCl_4 for 16 weeks (black arrow: fibrotic strands).

529 Fig. 5. Comparison of a typical *N*-glycan profile of a control, CCl_4 (F2-F4) and CBDL (F2-F4) mouse. The
530 peaks that significantly decrease in abundance compared to control mice are in red and those that
531 significantly increase in abundance compared to control mice are in green.

532 Fig. 6. The error bars represent the evolution of the FI in the progression towards cirrhosis. Starting
533 from a F2-stage, the FI is clearly higher in the CBDL mice (B) when compared to the CCl_4 mice (A).

534

535

536

537

538

539

540

541

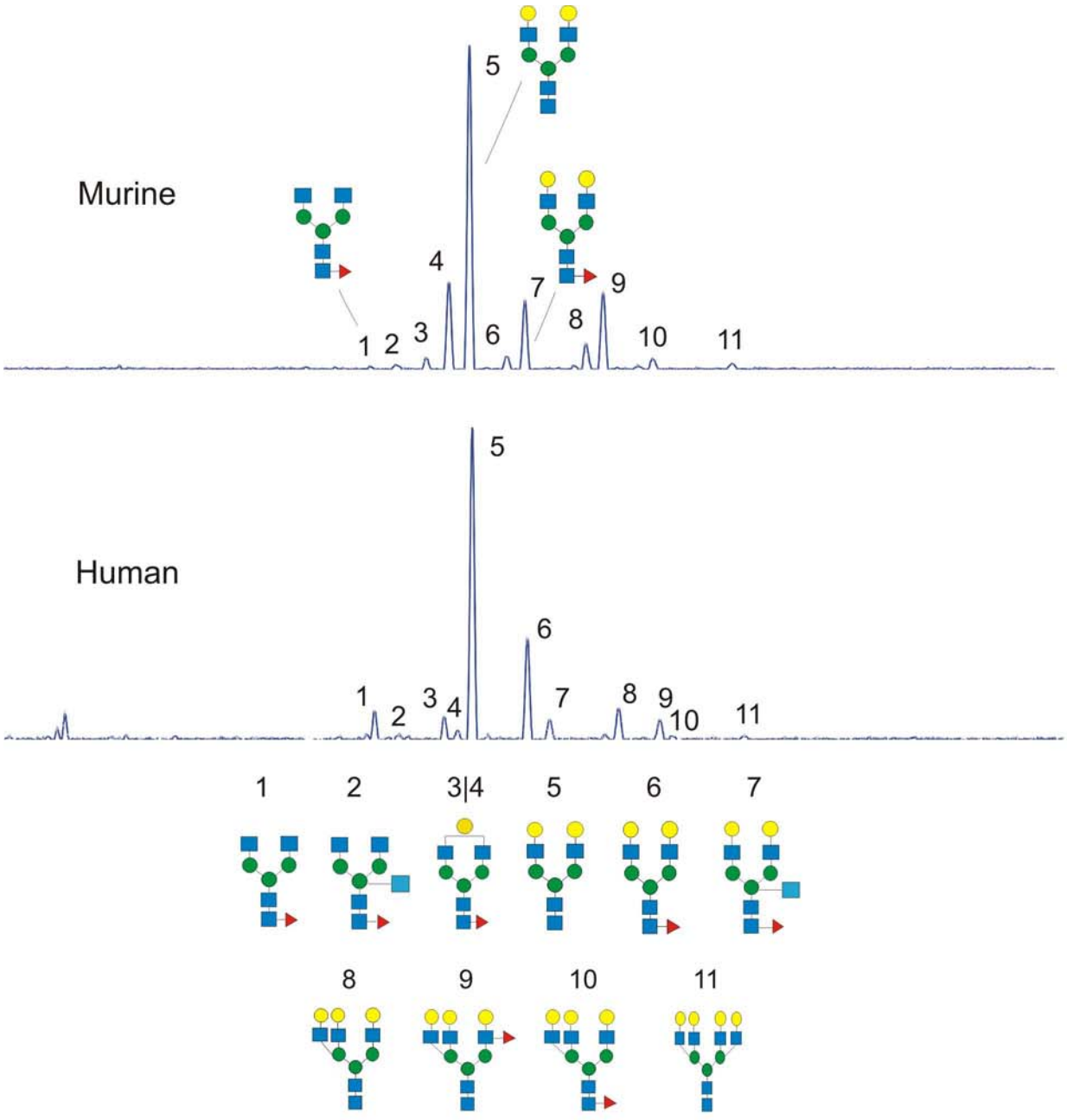
Murine
5
4
7
9
1
2
3
6
8
10
11
Human
5
6
1
2
3
4
7
8
9
10
11
1
2
3|4
5
6
7
8
9
10
11

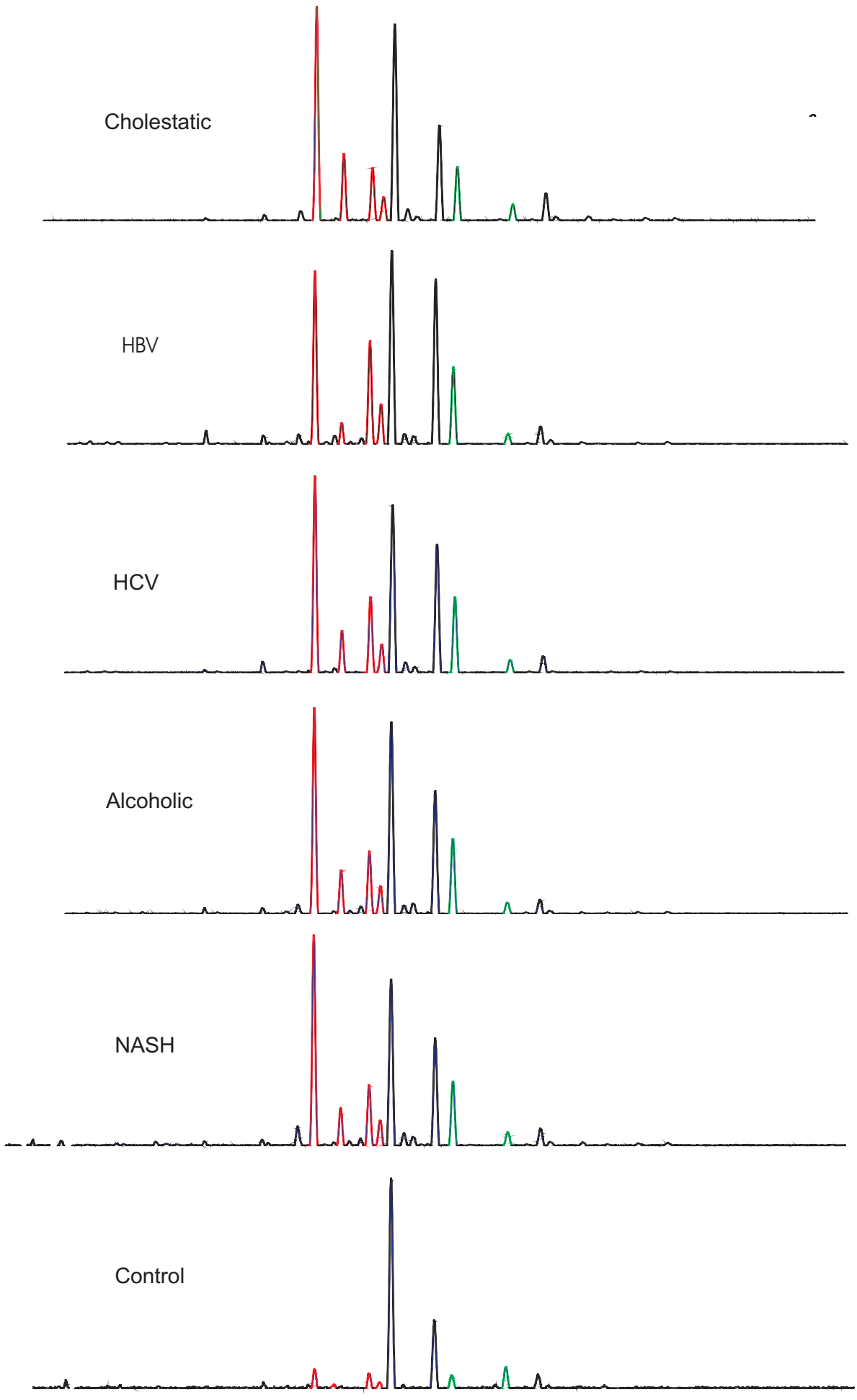
Cholestatic
HBV
HCV
Alcoholic
NASH
Control

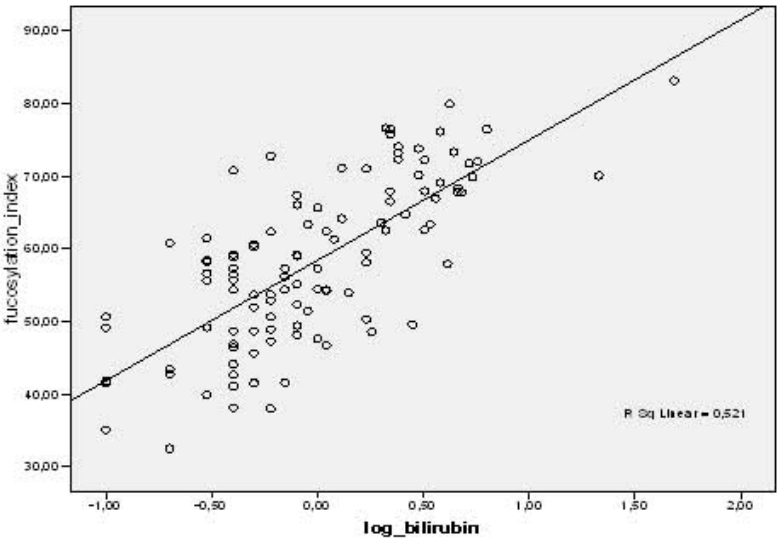
fucosylation_index
90,00
80,00
70,00
60,00
50,00
40,00
30,00
-1,00
-0,50
0,00
0,50
1,00
1,50
2,00
log_bilirubin
R Sq Linear = 0,521

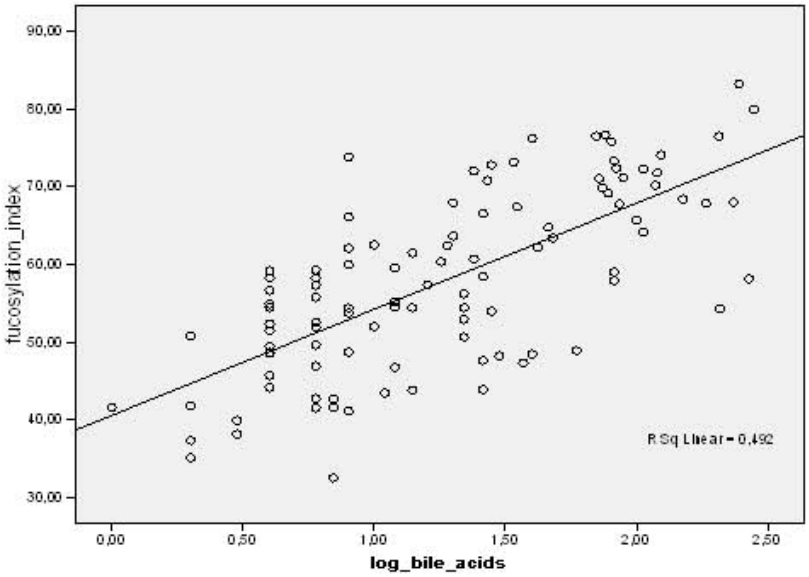
fucosylation_index
90,00
80,00
70,00
60,00
50,00
40,00
30,00
0,00
0,50
1,00
1,50
2,00
2,50
log_bile_acids
R Sq Linear = 0,492

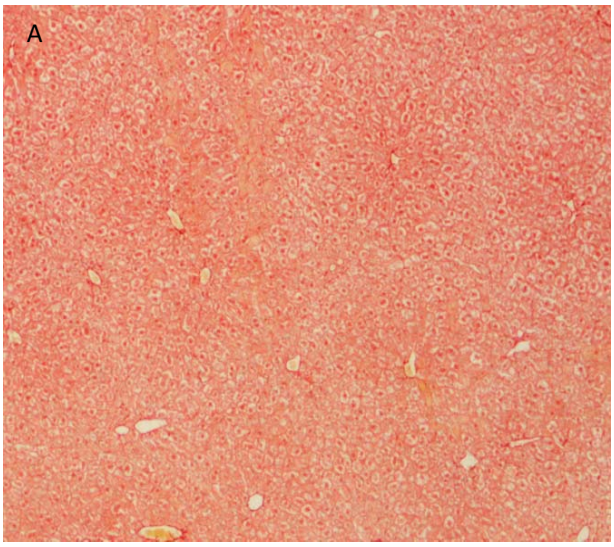
A

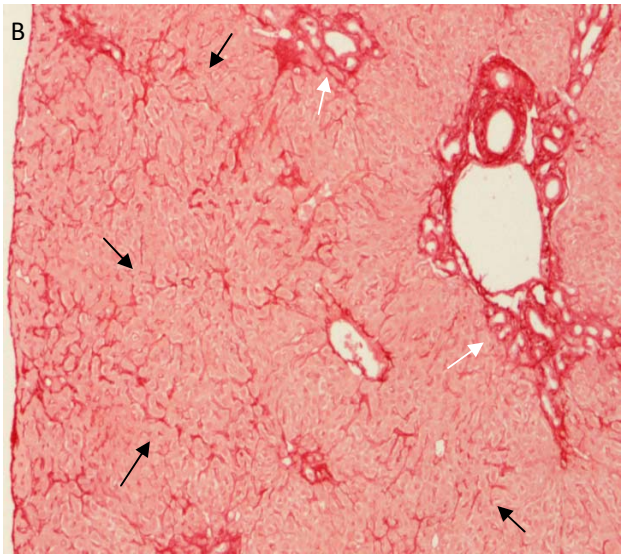
B

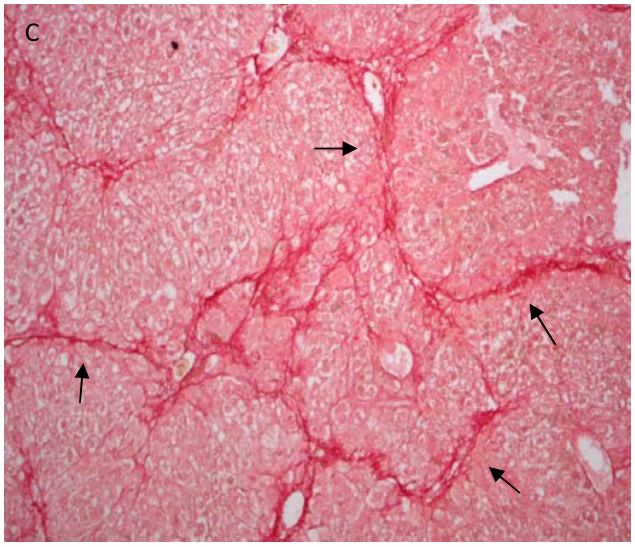
C

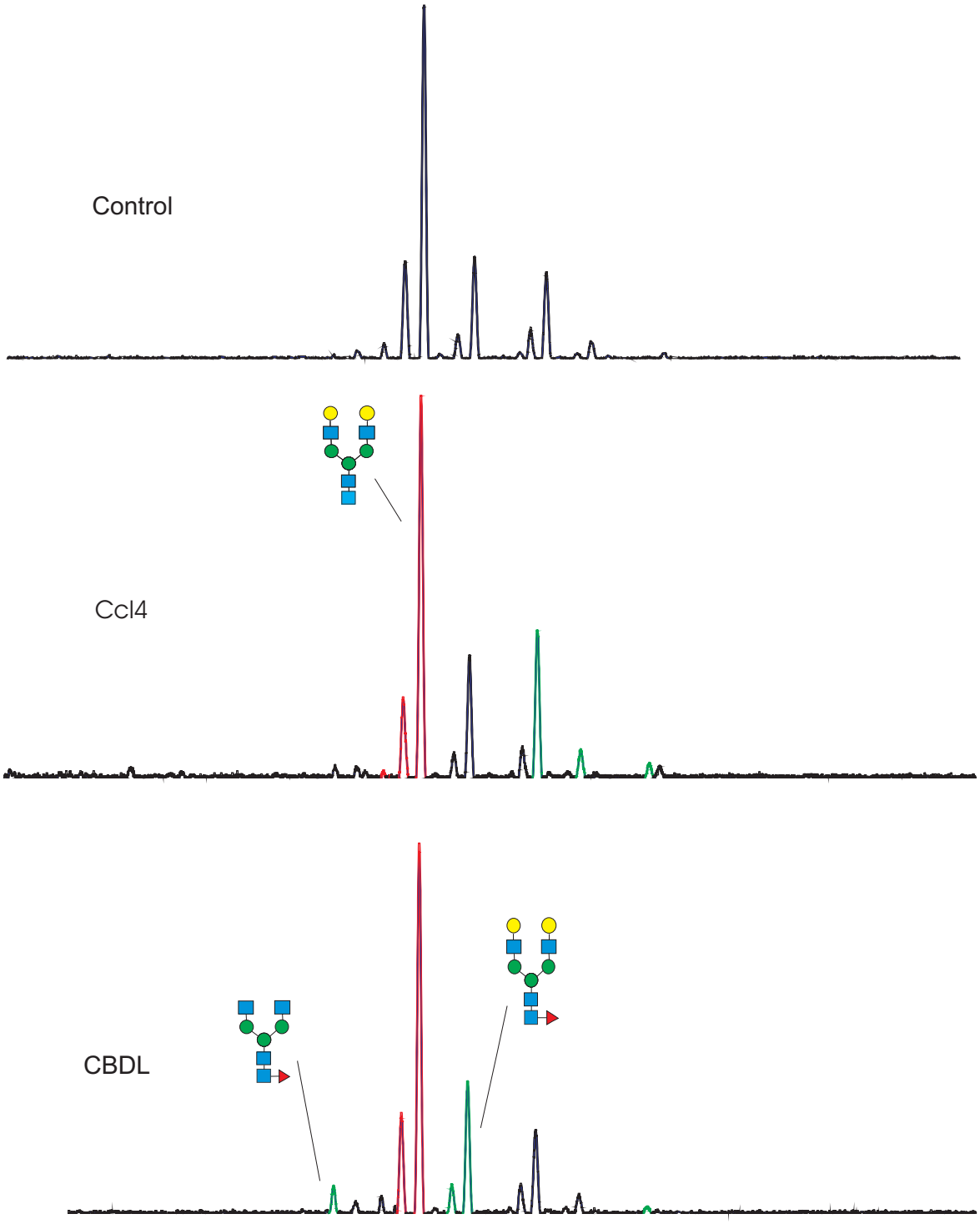
Control
Ccl4
CBDL

A

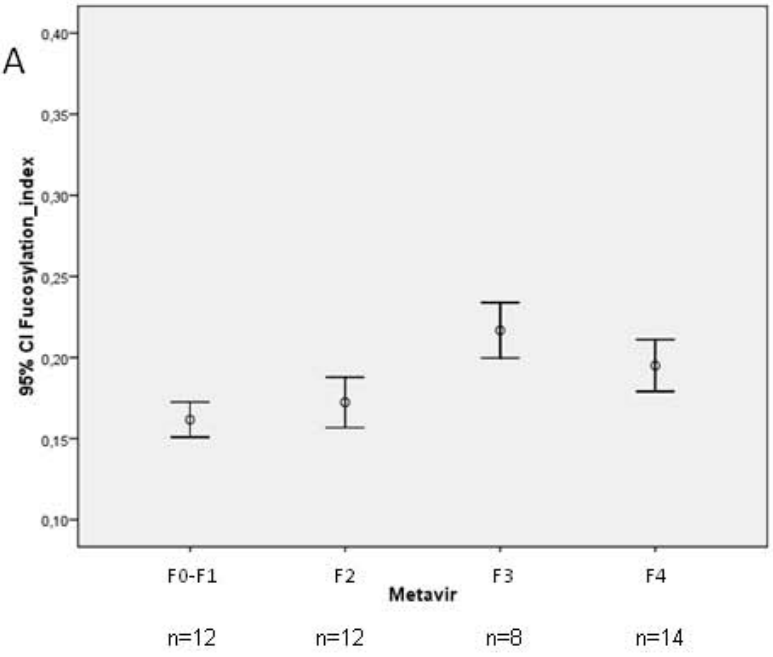

n=12 n=12 n=8 n=14

B

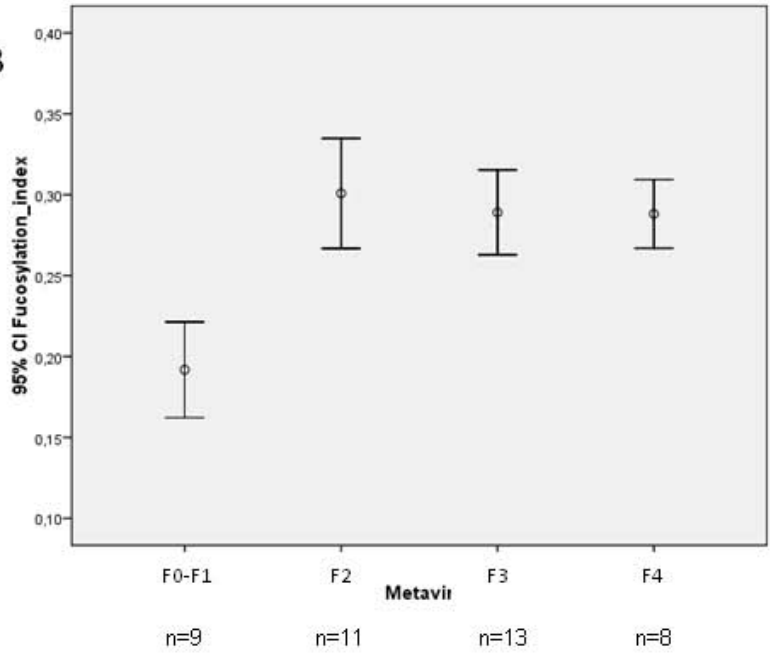

n=9 n=11 n=13 n=8

Table 1: Anthropomorphic data and liver tests in the different etiologies of chronic liver disease and control group

	Fibrosis/Cirrhosis-patients Etiologies					
	Cholestatic	HBV	HCV	alcoholic	NASH	control
Age (y)	45,2 (±15,6)	45,1 (±16,4)	53,9 (±16,1)	59,2 (±9,2)	46,2 (±12,2)	46,6 (±12,8)
Weight (kg)	72,9 (±14,8)	80,3 (±15,5)	72,9 (±13,6)	80 (±18,5)	89,4 (±23,7)	ND
Sex (m/f)	10/5	13/7	21/11	22/9	11/6	10/5
F0-F1	ND	ND	5/32 (15,6%)	ND	ND	NA
F2	ND	ND	3/32 (9,4%)	ND	ND	NA
F3	ND	ND	3/32 (9,4%)	ND	ND	NA
F4	4/15 (26,7%)	9/20 (45%)	21/32 (65,6%)	23/31 (74,2%)	4/17 (23,5%)	NA
Bilirubin (mg/dl)	1,34 (±1,5)	1,04 (±0,93)	1,02 (±1)	1,79 (±1,4)	5,3 (±14,4)	0,2 (±0,16)
AST (U/l)	45,6 (±39,6)	31,2 (±15,9)	68,3 (±42,8)	43,6 (±26,3)	34,8 (±38,4)	8,6 (±5,7)
ALT (U/l)	55,5 (±52,1)	33,1 (±31,2)	76,8 (±81,5)	31,3 (±19,2)	36,1 (±58,1)	10,6 (±3,9)
GGT (U/l)	202,3 (± 439)	24,8 (±13,7)	89,3 (±73,2)	117,5 (±115,8)	98 (±127,1)	29,2 (±24)

ND: Not Determined NA: Not Applicable

Table 2: Anthropomorphic data and liver tests in the different etiologies of HCC-patients

	Etiologies of HCC-patients			
	HBV	HCV	alcoholic	NASH
n	2	4	8	2
Age (y)	72 (±12,7)	76,3 (±7,6)	64,7 (±16)	65,5 (±78)
Weight (kg)	54,5 (±7,8)	69,5 (±17,7)	73,8 (±18,1)	83 (±8,9)
Sex (m/f)	1/1	3/1	5/3	1/1
Bilirubin (mg/dl)	3,4 (±4,1)	1,85 (±1,6)	5,1 (±6,9)	0,6 (±0)
AST (U/l)	76 (±84,9)	73,5 (±30,4)	70,1 (±59,3)	31,5 (±17,7)
ALT (U/l)	44,5 (±40,3)	64 (±24,2)	35 (±20,1)	37 (±14,1)
GGT (U/l)	99 (±46,7)	217,3 (±193,4)	164,4 (±83,4)	136 (±161,2)
AFP (ng/ml)	1009 (±1422)	133,1 (±208,9)	10027 (±24416,4)	140,1 (±195,1)
MELD score	13,9 (±5,8)	11,7 (±3,4)	14,2 (±8,4)	7,2 (±0,1)
Milan criteria (within/outside)	1/1	3/1	5/3	1/1

Table 3: laboratory tests: CBDL - Sham and CCl_4 - saline (n=8 per group)

	CBDL					Sham				
	1w	3w	6w	10w	16w	1w	3w	6w	10w	16w
AST (U/L)	586 (±417)	377 (±101)	326 (±75)	477 (±239)	422 (±201)	87 (±16)	102 (±52,5)	71 (±12)	82 (±34)	136 (±52)
	***	***	***	***	***					
ALT (U/L)	694 (±662)	246 (±38)	206 (±65)	296 (±118)	284 (±141)	66 (±39)	46 (±18)	41 (±12)	38 (±10)	68 (±44)
	***	***	***	***	***					
TBiln (mg/dl)	13,1 (±6,2)	24,8 (±4,9)	20,7 (±5,7)	17,6 (±4,6)	22,9 (±4,6)	0,11 (±0,04)	0,13 (±0,04)	0,12 (±0,02)	0,16 (±0,04)	0,19 (±0,03)
	***	***	***	***	***					
	CCl_4					Saline				
	1w	3w	6w	10w	16w	1w	3w	6w	10w	16w
AST (U/L)	112 (±42)	215 (±159)	78 (±44)	122 (±61)	98 (±26)	89 (±21)	81 (±23)	72 (±21)	87 (±81)	67 (±29)
		**			*					
ALT (U/L)	87 (±52)	68 (±24)	51 (±30)	77 (±28)	88 (±34)	81 (±59)	41 (±16)	38 (±6,9)	47 (±15)	28 (±10)
		**		*	**					
TBiln (mg/dl)	0,2 (±0,06)	0,17 (±0,05)	0,22 (±0,08)	0,21 (±0,15)	0,19 (±0,02)	0,2 (±0,2)	0,12 (±0,01)	0,15 (±0,04)	0,09 (±0,04)	0,21 (±0,05)
		**	*	*						

Mean (±SD); *p<0,05 ** p<0,01 *** p<0,001 compared to Sham and saline

Table 4: mean relative peak height (in %) of the different peaks in the mouse electropherogram (treated – control).

Group	Time point	Peak 1	Peak 2	Peak 3	Peak 4	Peak 5	Peak 6	Peak 7	Peak 8	Peak 9	Peak 10	Peak 11
CCl4 - Saline	Week 1	0,7-0,7	1,4-1,7	1,3-1,8	10-11,4	46,2-47,7	2,6-3,3	13,6-15,2	3,9-3,5	15,3-11,2 ***	3-2,7	1,6-1 ***
	Week 3	0,7-0,8	1,1-1,3	3-2	12,9-12,6	45,4-49,3 *	2,6-2,9	12,2-12,7	4,5-3,8	13,8-11,6 *	2,4-2,2	1,3-1 *
	Week 6	1,4-1,4	1,3-1,2	0,7-2,3 **	6,9-12,7 ***	49,2-48,3	2,5-2,9	16,2-12,4	2,3-4	15,2-11,7 **	3-2 ***	1,4-1 *
	Week 10	2-2,9	1,2-1,4	0,8-1,6 **	9,3-12,3 ***	45,9-48,8	3,2-3,4	14,6-13,2	3-3,2	15,9-10,7 ***	2,7-1,8 ***	1,5-0,8 ***
	Week 16	2,7-2,3	1,3-1,6 *	0,8-1,1 **	9,2-12,3 ***	44,6-50,9 ***	2,2-2,5	14,8-13,7	3-2,6	17,2-10,5 ***	2,5-1,8 **	1,7-0,8 ***
CBDL - Sham	Week 1	0,9-0,6 *	0,9-1,1	4,6-3,7	16,3-15,2	40,9-40,5	3,4-3,3	14-12	4,5-5,9 *	11,1-14 *	1,7-2,6	1,7-1,4 *
	Week 3	5,8-1,7 **	1,8-2,5	2,1-2,4	10,1-12,8 **	40-46,6 **	3,6-2,8 **	20,5-13 ***	2,5-4 ***	9,8-11 *	1,9-2,1	2-1 ***
	Week 4	3,3-2,3 *	1,3-1,2	2-1,3	10-10,5	43-51,2 ***	3,6-2,9 **	20,2-14,3 ***	2,5-2,8 *	9,9-11,2	1,9-2	1,7-0,7 ***
	Week 5	6,5-2,6 **	1,5-1,6	1,7-1,6	9,2-10,6	38,7-47,4 ***	3,2-3 *	21,3-15,6 ***	2,5-3,2 *	11,1-11,2	2,4-2,5	1,7-0,9 **
	Week 6	3,7-1 ***	1,7-1,2	1,3-1,5	10,5-14,9 ***	41-48,9 ***	3,8-3,5 *	20,9-13,2 ***	2,5-3,2 ***	11,1-9,9 *	2,4-2 **	2,1-0,8 ***
PPVL-Sham	Week 1	1,1-1,5	1,2-1,1	4,1-3,3	16-14,8	39-44,4 **	4,6-3,3 *	15,2-12,8	4,7-4,4	10,5-11,3	2,6-2,1	1,1-1
	Week 2	1,1-1,6	1,2-1,3	1,8-2,2	13,1-14	48,7-49,8	3,5-4	12,3-13,9	3,6-3,5	12-9,2 ***	1,7-1,9	1-0,8

*0,01<p<0,05 **p<0,01 ***p<0,001